COMPOSITE LANDING GEAR DESIGN PROCESS

Pavel Schoř **Jan Šplíchal** **Michal Mališ**

Institute of Aerospace Engineering
Faculty of Mechanical Engineering
Brno University of Technology

Technická 2896/2
616 69 Brno
Czech Republic

pavel.schor@email.cz splichal@fme.vutbr.cz michal.malis@centrum.cz

Abstract. A composite landing gear springs never became widely adopted by GA manufacturers. Nowadays these composite springs are going to be popular in light sport aircrafts. This article describes an experience gained during design process of landing gear for VUT-061 aircraft. Several methods were used including analytical models and FEM models. Although these models are well understood, the composite landing gear design can lead the designers into serious problems, since the design requires also some empirical methods and an analysis of drop test to be used. By employing of sandwich failure criterion, the successful design can be achieved. Composite post processing software COMPOST for NASTRAN FEM solver was developed to meet these requirements. The usefulness of the Compost-software was demonstrated after drop test of first landing gear for VUT-061. There a crushing failure occurred. This failure was predicted by the COMPOST software, but could not be predicted by 2D FEM shell model, which was originally used. Later, the compost software was extended by a 1D-beam FEM solver cmFEM (composite mini FEM). This speeded up the analysis process of new spring, which later passed the drop test. In this article we present a comparison of design methods, which were useful during design and analysis process from viewpoint of a light aircraft manufacturer or a homebuilder.

Keywords. FEM, Composite, Sandwich, Landing gear

1 Introduction

The VUT-061 is experimental turboprop powered aircraft designed according to CS-VLA regulation, maximum takeoff weight is 650kgs. It is further development of VUT-001(figure 1) and shares the same landing gear spring design.

The VUT-001`s landing gear spring was designed and tested at IAE-FME VUTBR test facility. As result of this process, lot of useable measurements was available for development of VUT-061 landing gear spring. Due design similarities of both aircraft, it was decided to use the same mold for landing gear spring for the VUT-061 as was used for the VUT-001. This also led us to the problems with a complicated geometry, since VUT-001`s spring is unusually wide and low height. This usually incorporates increased bending moments. The spring of the VUT-001 was designed piecewise linear, which resulted to delamination at folds. Moreover the VUT-061 was 50kgs heavier than VUT-001, counting 650kgs. It was decided to improve manufacturing technology of VUT-001 landing gear spring. This improvement led to two spring specimens till successful passing of the drop test.

Figure 1: VUT-001 Marabu, the predecessor of VUT-061 TURBO

Two spring landing gears for VUT -061 were designed. The VUT-061-01 spring landing gear overall characteristics were the same as on VUT-001. That gears were designed simply using analytical calculation. This specimen used glass fiber rowing in flanges, counting 15 layers per flange. Core was made of polystyrene foam. In this case, flanges and core were glued in a separate mold to achieve better fiber/resin ratio, which generally implies better strength properties. This specimen failed the drop test, approximate maximum y-force was 8378N. Posttest investigation revealed that geometrical characteristics were not fulfilled. Distance between flanges was around 1mm less, than required. Flanges were stiffened by glass fiber fabric webs. Table 1 shows one wheel reaction force measured at the drop test and maximum distance between upper clamped part of the gear and wheel axes in vertical direction. Moreover maximum vertical displacement including wheel tire deformation is referred.

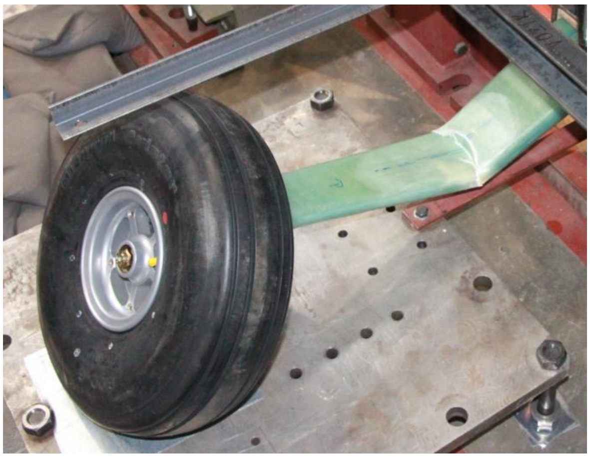

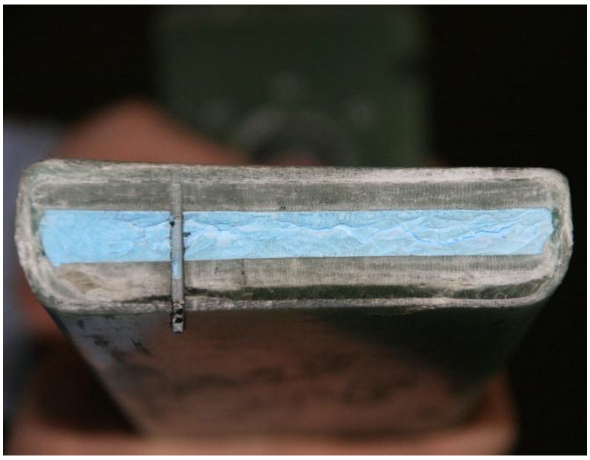

Figure 2: VUT-061 landing gear after unsuccessful drop test

Figure 3: Cross-section of gear at damaged point

Later investigation revealed that critical failure was sandwich core crushing and following debonding of upper flange from outer banding skin and compressive overloading of the foam core (figure 3). In that situation the composite sandwich beam lost structural compactness and collapse arose. (figure 2)
The second landing VUT-061-02 had a same geometry as spring specimen VUT-061-01. The flanges were reinforced, counting 16 layers per flange. Core material was changed to a Herex C70.90 foam, which had compressive strength of 1.9MPa. This specimen passed the drop test; maximum y-force was 10721N. Monitored characteristics of each specimen are mentioned in table 1.

Specimen	Measured vertical force [N]	Displacement at wheel axis [mm]	Displacement including tire deformation [mm]
VUT-061-01	8378	118	195,6
VUT-061-02	10721	107,59	208,7

Table 1: Drop tests – forces and displacements. [4]

2 Computational methods

Three different models were used to simulate failures occurred in landing gear structure at maximum loading during test: cmFEM - own simple 3D FEM model with 1D beam elements, 3D FEM model with 2D shell elements in NASTRAN, and full 3D model with QUAD elements in NASTRAN. Simplifications are explained on figure 4. Results from all models were compared to drop test results.

2.1 Simple linear 3D FEM model with 1D beam elements in cmFEM

A simple 3D FEM method was developed by authors with beam elements to be able to estimate overall stiffness of the landing gear spring. This method uses classic laminate theory to determine effective rigidities (2) from ABD matrices. These effective rigidities were used in element stiffness matrices (1); allow determining overall deformation and local element forces. From local element forces, moments and forces per unit length were recalculated as an input to the classic laminate theory to determine ply stresses. Unfortunately in case of specimen Spring VUT-061-01, only maximum ply stresses were checked. After the specimen failure during the drop test, additional sandwich failure criterions were employed to determine the cause of the failure. The evaluation showed increased failure indices in case of crushing failure.
Geometry, load, boundary conditions, layup and material properties used in this model are identical to 2D shell model, which is described below.

2.1.1 1D-Beam element formulation

This simple FEM method used standard 1D BEAM element in 3D space, which was taken from [3]. Element local stiffness matrix is defined as:

$$K = \begin{bmatrix} ra & 0 & 0 & 0 & 0 & 0 & -ra & 0 & 0 & 0 & 0 & 0 \\ 0 & rz3 & 0 & 0 & 0 & rz2 & 0 & -rz3 & 0 & 0 & 0 & rz2 \\ 0 & 0 & ry3 & 0 & -ry2 & 0 & 0 & 0 & -ry3 & 0 & -ry2 & 0 \\ 0 & 0 & 0 & rx & 0 & 0 & 0 & 0 & 0 & -rx & 0 & 0 \\ 0 & 0 & -ry2 & 0 & 2*ry & 0 & 0 & 0 & ry2 & 0 & ry & 0 \\ 0 & rz2 & 0 & 0 & 0 & 2*rz & 0 & -rz2 & 0 & 0 & 0 & rz \\ -ra & 0 & 0 & 0 & 0 & 0 & ra & 0 & 0 & 0 & 0 & 0 \\ 0 & -rz3 & 0 & 0 & 0 & -rz2 & 0 & rz3 & 0 & 0 & 0 & -rz2 \\ 0 & 0 & -ry3 & 0 & -ry2 & 0 & 0 & 0 & -ry3 & 0 & -ry2 & 0 \\ 0 & 0 & 0 & -rx & 0 & 0 & 0 & 0 & 0 & rx & 0 & 0 \\ 0 & 0 & -ry2 & 0 & ry & 0 & 0 & 0 & ry2 & 0 & 2*ry & 0 \\ 0 & rz2 & 0 & 0 & 0 & rz & 0 & -rz2 & 0 & 0 & 0 & 2*rz \end{bmatrix} \quad (1)$$

Where:

$$ra = \frac{Ex.A}{l} \qquad rx = \frac{G.J}{l} \qquad ry = \frac{2.Ex.Iy}{l} \qquad ry2 = \frac{6.Ex.Iy}{l^2} \qquad ry3 = \frac{12.Ex.Iy}{l^3}$$

$$rz = \frac{2.Ex.Iz}{l} \qquad rz2 = \frac{6.Ex.Iz}{l^2} \qquad ry3 = \frac{12.Ex.Iz}{l^3}$$

2.1.2 Effective bending stiffness, effective tensile stiffness

Since the beam uses a composite material, it is not possible to use standard engineering constants like A, Ex, Iy, Iz directly, because each layer can have different Young`s modulus Ex_i (3). This implies that contribution of each layer to overall bending stiffness is based on Ex_i Thus required bending stiffness is be calculated directly from layer properties and layer position as:

$$E.Iz = \sum_{i=1}^{n} Ex_i\,(w.\frac{t_i{}^3}{12} + w.t_i.zn_i{}^2) \qquad (2)$$

Where:

Ex_i - Effective Young`s modulus of i-th layer explained bellow
w - Width of composite element
t_i - Thickness of i-th layer

The bending stiffness $E.Iy$ and tensile stiffness $E.A$ can be obtained in similar manner. The effective Young`s modulus Ex_i of i-th layer is obtained from ABD matrix of single ply laminate, which consist only of i-th layer. It is calculated as:

$$Ex_i = \frac{1}{A_{1,1}{}^{-1}.t} \qquad (3)$$

Where:

$A_{1,1}{}^{-1}$ - In plane stiffness from inverted ABD matrix
t - Layer thickness

The Effective Young`s modulus of i-th layer Ex_i can be also obtained directly from CLT as $Qxyi_{1,1}$, where $Qxyi_{1,1}$ is stiffness matrix of i-th layer transformed to x-y coordinates.

2.2 3D FEM model with 2D shell elements in NASTRAN

The shell model of the spring is based on mid surface of the spring body. This mid surface is meshed with QUAD4 elements. Wheel axis was modeled by BAR2 elements and connection to the spring mid surface is done by RBE2 elements. This model was enhanced by a tire model with BAR2 elements. Properties of these elements were equal linear spring, which had the same rigidity as the real tire (figure 2).

Properties of each QUAD4 element were defined by MSC.PATRAN laminate modeler module.
A composite layup consists of 0° UD glass fiber flanges, which are wrapped by +-45° glass fiber fabrics. Simplifications according to the figure 4 were used.

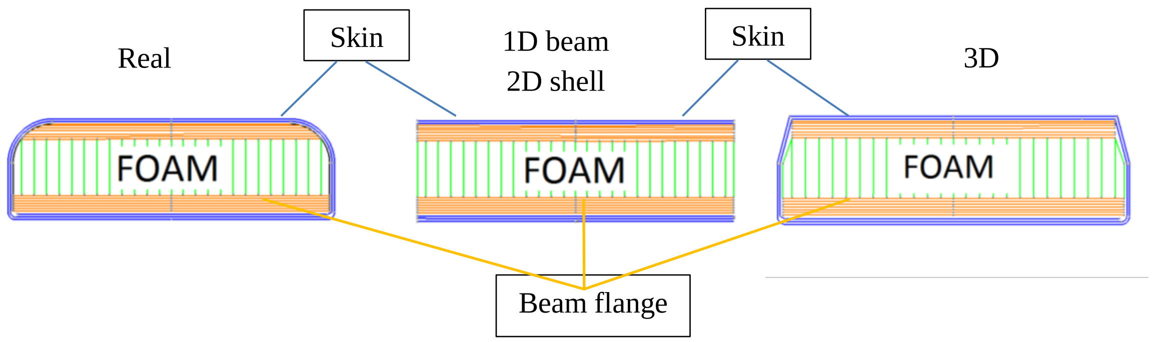

Figure 4: Comparison of real cross section and 1D beam, 2D shell and 3D FEM model.

2.2.1 Loads and boundary conditions

For both FEM models, the same boundary conditions were applied. Hence the task is symmetrical; only one half of the spring was modeled. Transitional displacements were restricted at location of the support. Symmetry boundary conditions were applied at symmetry plane.
The force was applied at wheel axis as shown on figure 5 and 6.

Figure 6: 2D element model load and boundary conditions

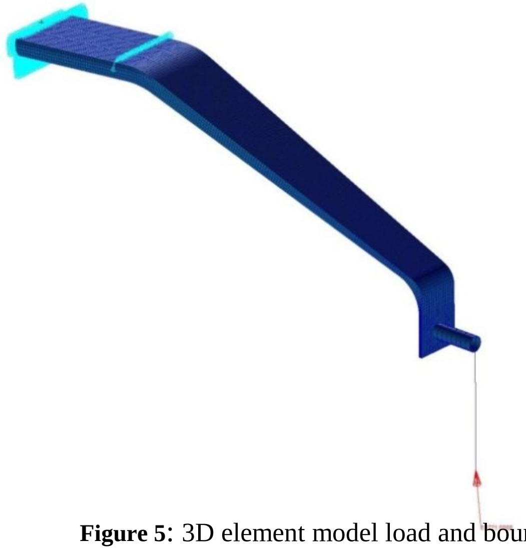

Figure 5: 3D element model load and boundary conditions

2.2.2 Material properties

Following material properties were used. Fiber/resin ration was estimated 0.35, therefore material properties of laminates were recalculated as shown in table 2.

	E_{11}	E_{22}	μ_{12}	G_{12}	G_{23}	G_{13}	t
	[MPa]	[MPa]	[-]	[MPa]	[MPa]	[MPa]	[mm]
92125	24900	24900	0,037	3800	1818	1818	0,16
UD glass 600 g/m^2	37332	6400	0,37	3600	3600	3600	0,4

Table 2: Material properties of flanges and wrap

The tension/ compression Young`s moduli were derived from compressive laboratory test according ASTM-C365-03. Shear Young`s moduli were modified in order to sandwich core shear stiffness was equal to global shear stiffness of landing gear. The shear modulus was reduced using (4), thus skin shear stiffens on the sides of landing gear was taking into account. This resulted into core properties mentioned in table 3.

$$G_{12,23,13} = G_{\#}\frac{2t}{B} + G_{core}\frac{B-2t}{B} \quad (4)$$

Where:
$G_{\#}$ - Effective shear Young`s modulus of landing gear side skin
t - The side skin
B - Landing gear width

	E_{11}	E_{22}	μ_{12}	G_{12}	G_{23}	G_{13}
	[MPa]	[MPa]	[-]	[MPa]	[MPa]	[MPa]
Herex foam	50	50	0,3	460	460	460

Table 3: Material properties of core in 1D-beam and 2D-shell models

2.3 3D model with QUAD elements in NASTRAN

This model consists of 3D FEM model of the core foam, 2D model of flanges, and 2D model of the wrap-around. Core is modeled using HEX8 elements, flanges and wrap-around are modeled by QUAD4 elements.

2.3.1 Material properties

Material properties of flanges and wrap were the same as used in 1D BEAM, and 2D shell models, but material properties of the foam were not modified as in case of 1D BEAM, and 2D shell models. Overall core properties are mentioned in table 4.

	E_{11}	E_{22}	μ_{12}	G_{12}	G_{23}	G_{13}
	[MPa]	[MPa]	[-]	[MPa]	[MPa]	[MPa]
Herex C70.90	50	50	0,3	19,23	19,23	19,23

Table 4: Material properties of core 3D model

3 Evaluation

Beams, which are not isotropic, can suffer on different failures, which are occurring very rarely in isotropic beams. In this article are briefly described only failure criterions, which could occur in composite landing gear.

3.1 Laminate ply failures

These failures are related to a single ply of laminate, which is examined independently. Strains are determined by the Classic Laminate Theory (CLT) for whole sandwich, while stresses in each layer depend on properties of each layer. Max stress failure criterion for composite materials plies is used. This failure criterion is described as a ratio of current stress and allowable stress in main fiber directions. Allowable stress, like other layer properties, depends on fiber/resin ratio of given layer. This failure criterion is usually used as the basic criterion at design stage, since it allows determining the required flanges layup.

3.2 Sandwich panel failures

Furthermore standard structural sandwich failure criteria are used for analyses evaluation. Flexural core crushing and transverse shear failure were selected as possible failures in composite material landing gear. Other standard sandwich failure criteria as a face sheet winkling, crimping or dimpling applied into COMPOST software suppose face sheet local buckling and was not considered. The local buckling of the landing gear flange made from thick laminate was assumed as highly unlike.

3.2.1 Flexural core crushing

Flexural core crushing [1] usually occurs during bending, when the bending moment is high and the core compressive strength is insufficient. The COMPOST software uses equation (5) to determine the core crushing failure:

$$FI = \frac{\frac{Mx^2}{d\,D_{1,1}} + \frac{My^2}{d\,D_{2,2}}}{\sigma_{Call}} \tag{5}$$

Where:

Mx, My	-	Applied bending moments per unit length
d	-	Distance between faces (flanges)
$D_{1,1}$, $D_{2,2}$	-	Bending stiffness from ABD matrix
σ_{Call}	-	Core compressive strength

3.2.2 Transverse shear failure

Transverse shear failure occurs when the core shear allowable strength is exceeded. When the design employs webs wrapped around the core and flanges, this failure is also unlikely to occur, since webs will carry more shear load, than the core. The COMPOST software uses equation (6) to determine the transverse shear failure:

$$FI = \frac{\sqrt{{\tau_{1,3}}^2 + {\tau_{2.3}}^2}}{\sigma_{Sall}} \tag{6}$$

Where:

$\tau_{1,3}, \tau_{2.3}$	-	Transverse shear stresses
σ_{Sall}	-	Core shear strength

4 Discussion

4.1 Result comparison

Both NASTRAN models used material and geometrical nonlinearities. Simple 1D model used linear material.

Displacements from all three FEM models are compared to the drop test result in table 5.

To evaluate Max stress failure criterion on the 2D model the COMPOST software was used. This software allows visualization of stresses in composite plies and determination of different failure criteria. Maximum stress values at upper bent are mentioned in table 6, while thru thickness σ_1 stress distribution at same place visualized by the COMPOST is shown on figure 7.

	Displacement at wheel axis [mm]	Displacement including tire deformation [mm]
1D beam model - linear	124	-
2D shell model - linear	118,9	255,06
2D shell model	95,56	213,48
3D shell model	100,81	207,92
Drop test [4]	107,59	208,7

Table 5: Displacement comparison

Maximum stresses σ_1 in fiber-direction in flanges:

	σ_1 Top flange [MPa]	σ_1 Bottom flange [Mpa]
2D shell model	-208,44	176,97
3D model	-235,11	124,23
1D beam model	-262,4	173,1

Table 6: Stress at upper bent

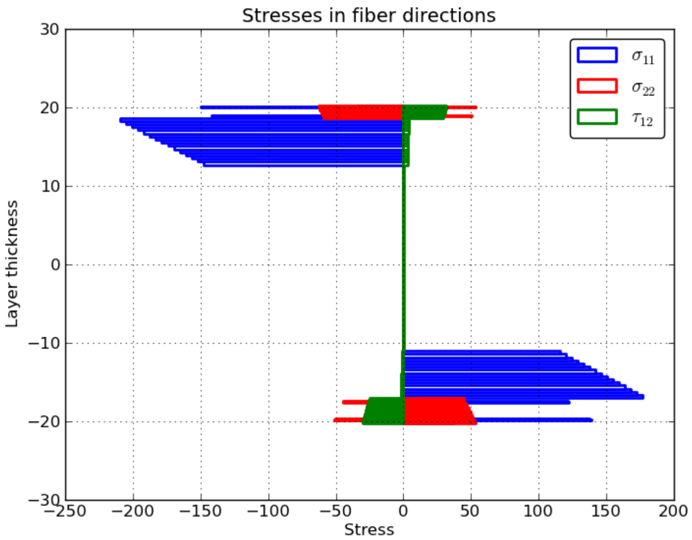

Figure 7: Example of stress distribution visualized by the COMPOST (for one element)

4.1.1 Core compressive stress

Core compressive stress can be evaluated directly from the 3D model of the core (figure 8), but the 2D model requires a post processing by COMPOST or similar software. In case of 1D model, the compressive stress was evaluated using flexural core crushing failure criterion (figure 9). Both results display through- thickness normal stress around 0.7MPa which exhibited compressive overloading of core and failure in case the first landing gear specimen VUT 061-01, which had core compressive though thickness allowable 0.5MPa.

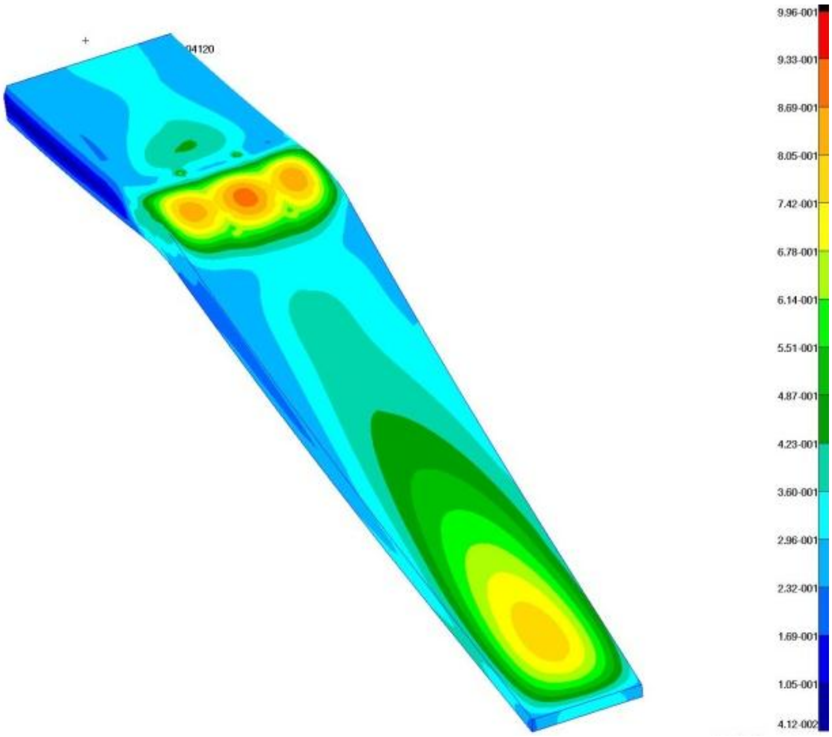

Figure 8: Von Misses stress results on foam 3D model

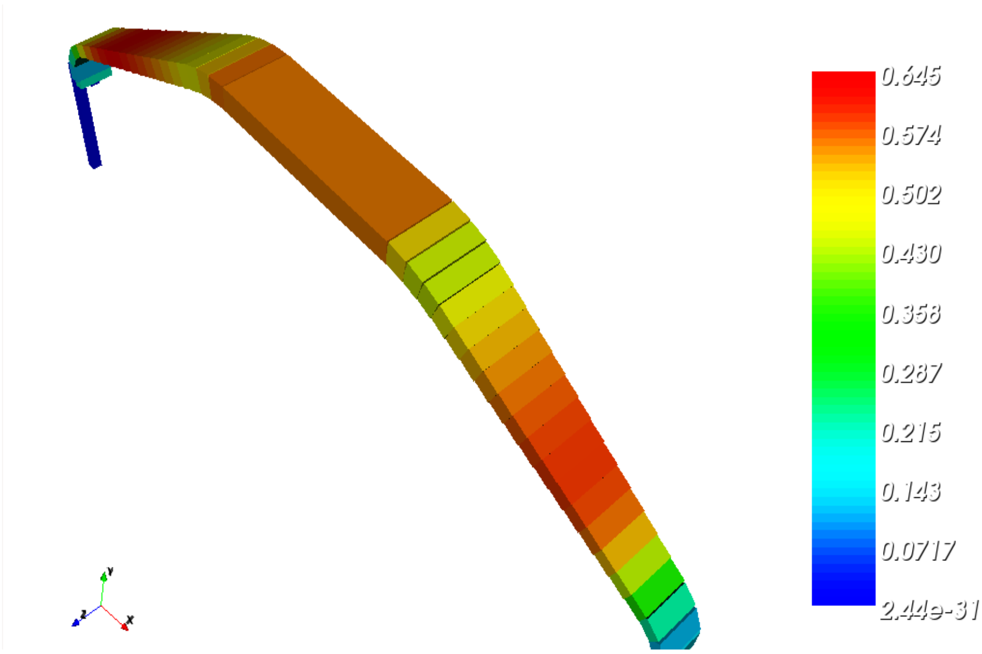

Figure 9: Through thickness normal stress in foam on 1D element model

4.1.2 Future work

We have shown that core compressive stress values were computed by 1D-Beam and 3D model with approximate the same accuracy. In this case, the geometrical nonlinearity plays important role during displacement calculation. This implies the need for simple non-linear solver for our simple FEM method. On the other hand, results obtained from simple FEM method seems to accurate enough for design purposes.
As shown on figure 8 – result from NASTRAN, at folds is also stress present. This phenomenon is called thru thickness normal stress and is known from curved beam theory. Future versions of our 1D-beam solver should incorporate this phenomenon, because it caused serious problems at VUT-001 landing gear development.

5 Conclusions

We suggest that for light aircraft manufacturers or home-builders it is not necessary to use detailed FEM models to achieve a successful landing gear spring design. By employing 1D BEAM FEM formulation, the designer is able to evaluate the spring sufficient accuracy and is still able to make effective design improvements. Moreover general purpose FEM solver and pre&post processors are usually not available for home-builders, yet these systems usually require experienced and well trained staff to obtain correct results. Our suggested method is not as complex as general purpose FEM system, but it can be understandable for the designer and as we suggest, it is also suited for this particular task. All of these findings can be used for future landing gear developments. While composite landing gear makes serious problems at design stage, it also offers a weight reduction in comparison with conventional metal landing gear. By solving the design problems, the composite landing gears may become used also by GA aircraft manufacturers.

References

[1] D.B. Miracle and S.L. Donaldson.: ASM Handbook Volume 21: Composites, ISBN 978-0-87170-703-1

[2] FAA, Comparative Evaluation of Failure Analysis Methods for Composite Laminates /FAA/AR-95/109

[3] Introduction to Finite Element Methods: http://www.colorado.edu/engineering/cas/courses.d/IFEM.d/

[4] F. Vaněk : Report from VUT-061 main landing gear drop test, Internal report IAE FME BUT 2012